A-38 HOW TO CHOOSE A SUBSET OF FREQUENCIES FOR FREQUENCY-DOMAIN FINITE-DIFFERENCE MIGRATION

R.-E. PLESSIX and W.A. MULDER

Shell International E&P, PO Box 60, 2280 AB Rijswijk, The Netherlands

Abstract

Frequency-domain finite-difference migration can be accelerated by an order of magnitude if a subset of the available data frequencies is used. To avoid unwanted artefacts, the choice of this subset should be guided by two principles: sufficient localisation of reflectors and the avoidance of wrap-around. The first is related to the spatial resolution and Heisenberg's principle. The second is needed to avoid repetitive patterns and is related to the Nyquist sampling theorem. Here we study both by a simple analytical and a more complex 2D synthetic example.

Introduction

Finite-difference migration with the two-way wave equation can be accelerated by an order of magnitude if the frequency domain rather than the time domain is used. This gain is mainly accomplished by using a subset of the available frequencies. The implicit assumption is that the data have a certain amount of redundancy in the frequency domain [1][2][3].

The choice of frequencies cannot be arbitrary. Even for noise-free data, two criteria must be taken into account. The first is related to the localisation or resolution of reflectors in the migration image [1][2]. Here the equivalent of Heisenberg's principle plays a role. The second criterion is the equivalent of Nyquist's theorem. For regular time series, the theorem gives the condition under which wrap-around – or aliasing or periodic repetition – can be avoided. Wrap-around may also show up in depth migration, albeit in a more subtle way. Because migration involves propagation in a given background velocity model and summation over shots and receivers, the effects of wrap-around may disappear even when the Nyquist theorem is not obeyed.

We have studied these effects analytically for the constant-velocity case and determined sampling conditions that avoid wrap-around artefacts. A two-dimensional example has been used to test the validity of these conditions for a more realistic velocity model.

Analytical study

Basic equations

For simplicity we consider a horizontally layered medium with constant velocity v and reflectivity $r(z)$. Let the observed data be $d_{\mathrm{s,r}}(\omega)$ for a shot s and receiver r at a frequency $f = \omega/(2\pi)$. Synthetic data can be obtained by using the Born approximation $c_{\mathrm{s,r}}(\omega) = \sum_z r(z)s(\omega)\,e^{i\omega\tau_{\mathrm{s,r}}(z)}$, with $\tau_{\mathrm{s,r}}(\omega)$ the travel time from source s to sub point z to receiver r and $s(\omega)$ the (scaled) source strength. For an offset of $2h$, we have $\tau_{\mathrm{s,r}}(z) = \tau(z,h) = v^{-1}\left(z^2 + h^2\right)^{1/2}$. Amplitude effects have been ignored. If migration is viewed as the gradient of a least-squares fit to the data, we find from the cost function

$$J(r) = \tfrac{1}{2}\sum_{\omega}\sum_{\mathrm{s,r}}\left|c_{\mathrm{s,r}}(\omega) - d_{\mathrm{s,r}}(\omega)\right|^2, \tag{1}$$

the gradient with respect to the unknown reflectivity $r(z)$:

$$g(z) = \frac{\partial J}{\partial r}(z) = \mathrm{Re}\sum_{\omega}\sum_{\mathrm{s,r}} \bar{s}(\omega) e^{-i\omega\tau_{\mathrm{s,r}}(z)} \left(c_{\mathrm{s,r}}(\omega) - d_{\mathrm{s,r}}(\omega)\right), \tag{2}$$

Here $\bar{s}$ denotes the conjugate of s. The Hessian of the cost function is given by

$$H(z,z') = \mathrm{Re}\sum_{\omega}\sum_{\mathrm{s,r}} \left|\mathrm{s}(\omega)\right|^2 e^{-i\omega\left[\tau_{\mathrm{s,r}}(z)-\tau_{\mathrm{s,r}}(z')\right]}, \tag{3}$$

for observed data obeying $d_{\mathrm{s,r}}(\omega) = \sum_z \tilde{r}(z) s(\omega) e^{i\omega\tau_{\mathrm{s,r}}(z)}$. Note that $g(z) = \sum_{z'} H(z,z')\left[r(z') - \tilde{r}(z')\right]$.

Ideally, the Hessian is non-zero for $z = z'$ and zero otherwise. In general, this is not true and artefacts will show up in the migration image. The question is: can we suppress artefacts by judiciously choosing a set of frequencies?

Localisation

If we assume a continuous spectrum, a single event due to a reflector at $z = z_1$, and $s(\omega) = 1$, the summation over the frequencies in Eq.(3) can be replaced by integration, leading to

$$g(z) = \frac{2}{\Delta\tau(z)} \sin\left(\pi\Delta\tau(z)\left[f_{\max} - f_{\min}\right]\right)\cos\left(\pi\Delta\tau(z)\left[f_{\max} + f_{\min}\right]\right), \tag{4}$$

where the frequencies range from $f_{\min}$ to $f_{\max}$ and $\Delta\tau = \tau(h,z) - \tau(h,z_1)$. This represents the product of a rapidly and a slowly oscillating function. The localisation or resolution power can be measured by the size Δz of the main lobe of the sine, obeying $\pi\Delta\tau(h, z_1 + \Delta z)\left[f_{\max} - f_{\min}\right] = \pi$, resulting in $\Delta z \cong \frac{1}{2} v \sqrt{1 + (h/z_1)^2} \Big/ (f_{\max} - f_{\min})$ under the assumption that $\Delta z^2 << z_1^2 + h^2$. This represents Heisenberg's principle. Note that the result is valid at a single fixed offset $2h$ and that we have assumed that the summation can be replaced by integration. This requires at least a continuous range of frequencies, without "holes". A necessary condition to accomplish this has been given in [2] and reads

$$f_{m+1} = f_m / \alpha, \qquad \alpha = z_1 \Big/ \sqrt{z_1^2 + h_{\max}^2}, \tag{5}$$

for a set of frequencies $f_1 = f_{\min}, f_2, \ldots, f_{\mathrm{N}} = f_{\max}$ and half-offsets ranging from 0 to $h_{\max}$. Note that Eq.(5) implicitly defines a constraint on the interval between subsequent frequencies.

Wrap-around

Wrap-around occurs if one event is migrated to multiple sub points, so if $H(z_1, z') = H(z, z')$, for $z_1 \neq z$ and all z'. This happens if

$$2\frac{\omega}{v}\left(\sqrt{z_1^2 + h^2} - \sqrt{(z')^2 + h^2}\right) = \pm 2\frac{\omega}{v}\left(\sqrt{z^2 + h^2} - \sqrt{(z')^2 + h^2}\right) + 2\pi n, \tag{6}$$

for any integer n and for all z'. The minus choice of the $\pm$ sign leads to an equation that cannot be satisfied for all z'. For the plus choice, we consider an equidistant set of frequencies $f_m = m\, df$, m integer. With $\omega = 2\pi m\, df$ and $n = mp$, wrap-around occurs if

$$\tfrac{1}{2} pv/(2\, df) = \sqrt{z_1^2 + h^2} - \sqrt{z^2 + h^2}\,. \tag{7}$$

If z and z_1 are required to lie in the interval $[0, z_{\max}]$, we can avoid the wrap-around for

$$df \leq \tfrac{1}{2} v \Big/ \left(\sqrt{z_{\max}^2 + h^2} - h\right). \tag{8}$$

For $h = 0$ and $z_{\max} = \frac{1}{2}\, v\, T_{\max}$, where $T_{\max}$ is the time range of the data, we recover the condition given by Nyquist's theorem: $df \leq 1/T_{\max}$. With non-zero offsets, the bound on df increases favourably.

Figure 1 illustrates the above for 2 s of zero-offset data, using a 2 km deep model with a reflector at 1.2 km depth and a constant velocity of 2 km/s. The Nyquist theorem dictates a sampling of $df = 0.5$ Hz and a $z_{\max}$ of 2 km. Figure 1a has been obtained with these conditions. In Fig. 1b, the condition on $z_{\max}$ is violated, and the reflector is repeated at 3.2 km depth. This corresponds to $p = 1$ in Eq.(7). In Fig. 1c, condition (8) is violated and an artefacts occurs at 0.2 km, corresponding to $p = -1$.

The effect of stacking multiple-offset data is illustrated in Fig. 2, using the same model. Offsets range from 0 to 500 m at 50 m increment. Fig. 2a obeys the requirements and the image does not have artefacts. With $z_{\max}$ kept at 2 km, Eq.(8) dictates $df \leq 0.64$ Hz. Nevertheless, Fig. 2b that is computed with $df = 1$ Hz does not appear to suffer strongly from artefacts. The reason is that we only have a single reflector at 1.2 km depth, and that for this special case, Eq.(7) does not produce artefacts. Indeed, if we evaluate Eq.(8) with $z_{\max} = 1.2$ km, the depth of the reflector, we obtain $df \leq 1.25$ Hz. For higher values of df, we obtain the artefacts shown in Fig. 2c and 2d. Their amplitudes are smaller than that of the true event because of the stacking, but stacking is not sufficient to remove them. Figure 3 illustrates the effect of stacking in another way.

Iterations

Iterative migration [3] is another way of reducing the amplitudes of artefacts. A gradient-based optimisation algorithm can be used to minimise the cost function (1). This avoids the explicit computation of the inverse of the Hessian, as the latter is computationally out of reach for most problems. In the present case, however, we can compute the Hessian and check its condition number to see if iterative migration makes sense. If the condition number is reasonable, say around 100, its inverse exists and iterative migration will improve the image. If the condition number is very large, the Hessian is nearly singular and iterative migration may fail. Figure 4 shows the condition number as a function of the maximum offset for various choices of df. For 0.5 Hz, the matrix is well behaved. For larger values of df, we see that the curves approach the 0.5 Hz case for sufficiently large offsets. We expect iterative migration to be beneficial in those cases.

2D synthetic example

To test the validity of our criteria, a less trivial model was chosen. Time domain data were generated for the velocity model shown in Fig. 5. A marine acquisition with 351 shots and 157 receivers per shot, spaced at 25 m was used for 3 seconds of data per trace. Nyquist requires $df = 0.33$ Hz for zero-offset data and 0.84 Hz for the larges offset of 4 km, so $h_{\max} = 2$ km. Frequencies between 18 and 30 Hz have been used to obtain the migration images shown in Figs. 6 and 7, which look fairly similar. However, if only Eq.(5) is used, we obtain the image shown in Fig. 8, which clearly suffers from artefacts. Iterative migration will generally improve the result, as shown in [3].

Conclusions

We have determined conditions on the choice of frequencies to be used in frequency-domain finite-difference migration, assuming noise-free data. The conditions depend on the velocity, depth of the migration grid, and offset range. They show that the spacing between subsequent frequencies can be larger than the inverse of the time range prescribed by the Nyquist theorem, but is generally smaller than based on resolution arguments.

References

[1] Freudenreich, Y. and Singh, S., 2000, Full waveform inversion for seismic data - frequency versus time domain, 62nd Mtg.: Eur. Assn. Geosci. Eng., Session:C0054.

[2] Sirgue, L. and Pratt, R.G., 2001, An optimal choice of temporal frequencies for imaging: application to waveform inversion, 71st Ann. Internat. Mtg: Soc. of Expl. Geophys., 698–701.

[3] Plessix, R.-E., Mulder, W.A., and Pratt, R.G., 2001, Frequency-domain finite-difference migration with only a few frequencies? 71st Ann. Internat. Mtg: Soc. of Expl. Geophys., 1103–1106.

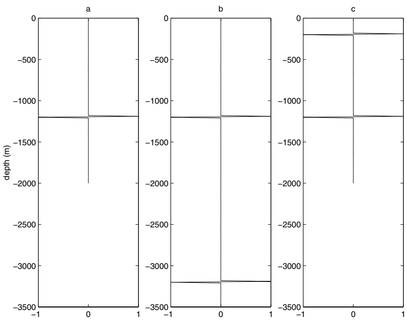

Figure 1. Migration images for zero offset data with a true event at 1.2 km depth, for **(a)** *df* = 0.5 Hz and a maximum depth of 2 km, for **(b)** *df* = 0.5 Hz and 3.5 km, and **(c)** *df* = 1.0 Hz and 2 km.

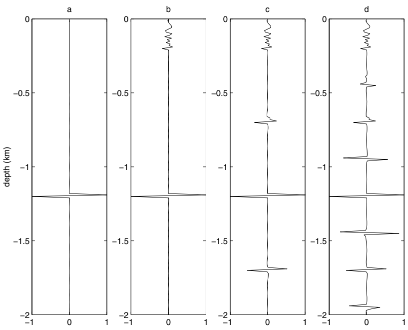

Figure 2. Migration images of multi-offset data for **(a)** *df* = 0.5, **(b)** 1.0, **(c)** 2.0, and **(d)** 4.0 Hz.

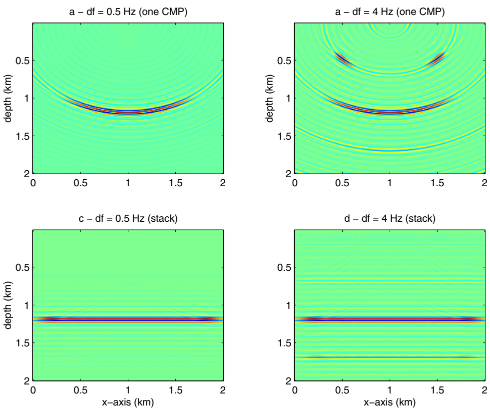

Figure 3. Migration results for *df* = 0.5 Hz (left) and *df* = 1.0 Hz (right) for one CMP (top) and after stacking 100 CMPs (bottom).

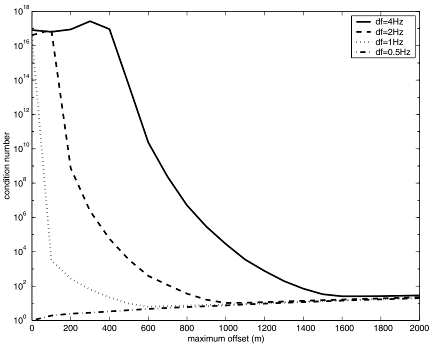

Figure 4. Condition number of the Hessian as a function of maximum offset for different frequency increments.

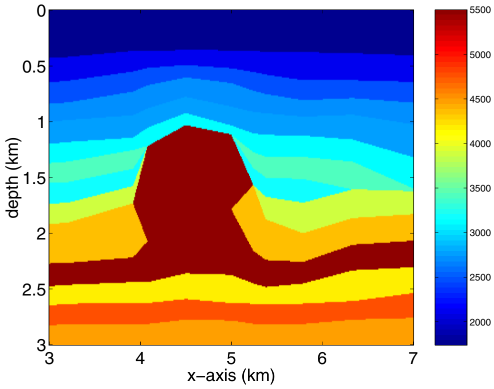

Figure 5. Central part of the velocity model.

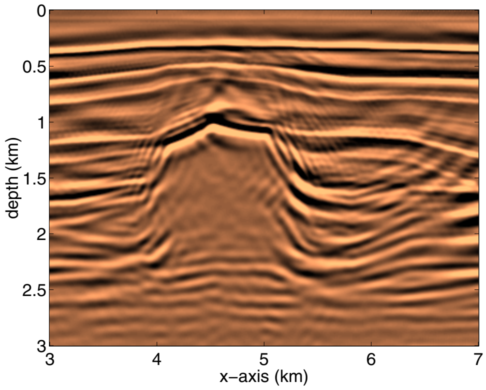

Figure 6. Migration image for *df* = 0.3 Hz.

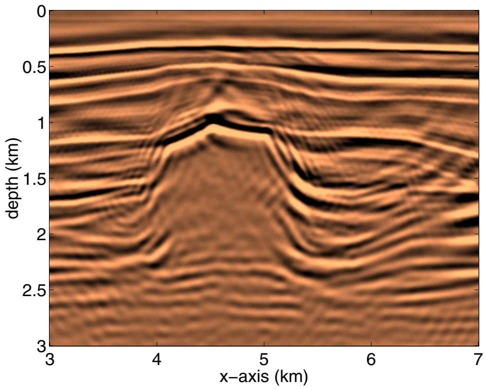

Figure 7. Migration image for *df* = 0.9 Hz.

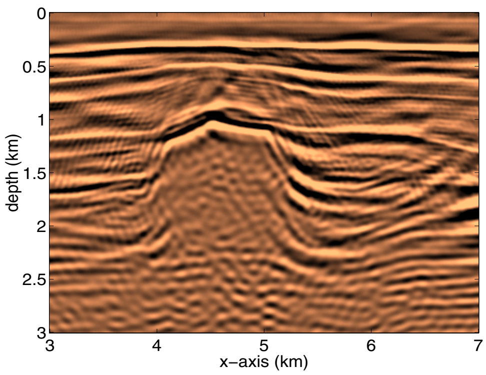

Figure 8. Migration image using 18, 21.6, 25.8, and 30 Hz.